

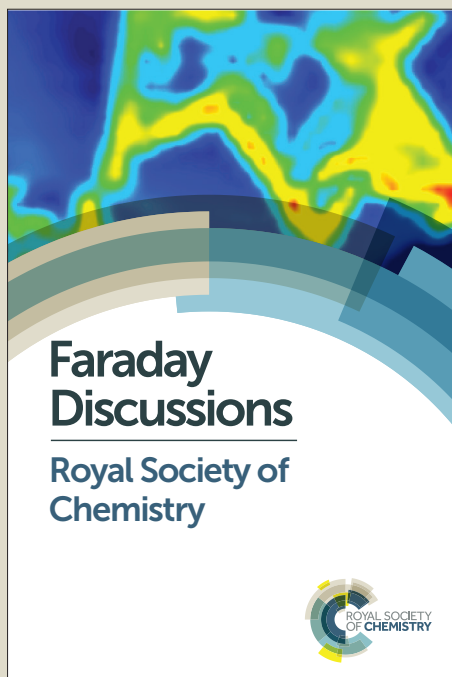
Faraday Discussions

Accepted Manuscript



This manuscript will be presented and discussed at a forthcoming Faraday Discussion meeting. All delegates can contribute to the discussion which will be included in the final volume.

Register now to attend! Full details of all upcoming meetings: <http://rsc.li/fd-upcoming-meetings>



This is an *Accepted Manuscript*, which has been through the Royal Society of Chemistry peer review process and has been accepted for publication.

Accepted Manuscripts are published online shortly after acceptance, before technical editing, formatting and proof reading. Using this free service, authors can make their results available to the community, in citable form, before we publish the edited article. We will replace this *Accepted Manuscript* with the edited and formatted *Advance Article* as soon as it is available.

You can find more information about *Accepted Manuscripts* in the [Information for Authors](#).

Please note that technical editing may introduce minor changes to the text and/or graphics, which may alter content. The journal's standard [Terms & Conditions](#) and the [Ethical guidelines](#) still apply. In no event shall the Royal Society of Chemistry be held responsible for any errors or omissions in this *Accepted Manuscript* or any consequences arising from the use of any information it contains.

Modelling the stochastic behaviour of primary nucleation

Giovanni Maria Maggioni^a and Marco Mazzotti^a

Received Xth XXXXXXXXXXXX 20XX, Accepted Xth XXXXXXXXXXXX 20XX

First published on the web Xth XXXXXXXXXXXX 200X

DOI: 10.1039/c000000x

We study the stochastic nature of primary nucleation and how it manifests itself in a crystallisation process at different scales and under different operating conditions. Such characteristic of nucleation is evident in many experiments where detection times of crystals are not identical, despite identical experimental conditions, but are distributed around an average value. While abundant experimental evidence has been reported in the literature, a clear theoretical understanding and an appropriate modelling of this feature is still missing. In this contribution, we present two models describing a batch cooling crystallisation, where the interplay between stochastic nucleation and deterministic crystal growth is described differently. The nucleation and growth rate of the two models are estimated by a comprehensive set of measurements of paracetamol crystallisation from aqueous solution in a 1 mL vessel [Kadam *et al.*, *Chemical Engineering Science*, 2012, **72**, 10-19]. Both models are applied to the cooling crystallisation process above under different operating conditions, i.e. different volumes, initial concentrations, cooling rates. The advantages and disadvantages of the two approaches are illustrated and discussed, with particular reference to the use across scales of nucleation rate measured in very small crystallisers.

1 Introduction

The importance of being able to describe and predict the course of primary nucleation in crystallisation processes cannot be overestimated. This is however challenging, both because monitoring and characterizing nucleation events is experimentally always difficult, and because scaling up information and models obtained in the lab to the scale of industrial processes results to be often not accurate enough.

Critical nuclei and sub-critical clusters are in fact nano-scale objects, which can normally be detected not when formed upon nucleation, but only after growing to a size large enough to occupy a significant volume fraction of the suspension. Hence, the detection (or induction) time, t_d , follows the nucleation time, t_n , of a time interval that depends not only on the nucleation rate but also on the growth rate, i.e. the speed at which newly formed nuclei grow while consuming the solute in the mother liquor.

^a *ETH Zurich, Institute of Process Engineering, Sonneggstrasse 3, Zurich, Switzerland. Tel: ++41 44 632 24 56; fax: ++41 44 632 11 41; email: marco.mazzotti@ipe.mavt.ethz.ch*

Moreover nucleation is on the one hand affected by mixing, heat transfer limitations and materials, whose characteristics vary when scaling up, and on the other hand exhibits poor reproducibility, in ways that are difficult to rationalise and control.

There are two interpretations of such poor reproducibility. When viewing nucleation and growth as deterministic phenomena, this is attributed to a high sensitivity to experimental conditions, which are difficult to reproduce exactly in repeated experiments. Such difficulty is well known to experimentalists, and is indeed an issue to be taken in serious consideration.

Otherwise, variability in the outcome of nucleation experiments is attributed to an intrinsic stochastic behaviour in the formation of critical nuclei, of which there is abundant experimental evidence (see the references reported in Table 1). This manifests itself as the fact that nucleation times (or induction times) are distributed statistically when many identical experiments are repeated, i.e. something that is typically possible only using vessels of very small size, namely in the nanolitre to millilitre range.

The conventional interpretation is that the formation of a critical nucleus is a rare event, which can be classified as a Poisson process. As a consequence, the number of nuclei obeys a Poisson distribution, and the nucleation times are accordingly distributed as follows:

$$P(t) = 1 - \exp\left(-\int_0^t k(t')dt'\right) \quad (1)$$

where t is time; $P(t)$ is the probability that nucleation (the formation of the first stable nucleus) occurs between $t = 0$ and t ; and $k(t)$ is the rate constant of the Poisson process, which is called homogeneous if k is time independent and inhomogeneous otherwise. The rate constant k multiplied by a generic time interval Δt gives the probability that an event, i.e. the formation of a new nucleus, occurs in that time interval. Note that in the previous equation as well as in the following ones, we assume that the system is saturated or supersaturated from $t = 0$ on.

In the present context k equals the product of the volume of the solution, V , where nucleation can occur, and of the rate of nucleation, J , given in number of particles per unit time and unit volume, e.g. as derived within the classical nucleation theory (CNT). A homogeneous Poisson process corresponds to nucleating a solution at constant volume V and constant nucleation rate, J , i.e. constant supersaturation and constant temperature. An inhomogeneous Poisson process corresponds to nucleation triggered by cooling of the solution or solvent evaporation, i.e. under conditions where supersaturation or temperature or volume or combinations thereof change in time. The average nucleation time, t_n^{avg} , and the standard deviation of its distribution, s_n , are calculated through the moments of the derivative dP/dt of the cumulative distribution (1) as:

$$t_n^{avg} = \int_0^\infty tk(t) \exp\left(-\int_0^t k(t')dt'\right) dt \quad (2)$$

$$s_n = \left(\int_0^\infty (t - t_n^{avg})^2 k(t) \exp\left(-\int_0^t k(t')dt'\right) dt\right)^{1/2} \quad (3)$$

Note that in the case of a homogeneous Poisson process $t_n^{avg} = s_n = 1/k =$

Table 1 Overview of relevant literature on stochastic nucleation from solution and the key features of each study. The category “Stochastic process” applies to the cases where stochastic nucleation is observed but no further specification about its nature is provided.

<i>Literature Overview</i>				
Reference	Technique	Volume	Detection	Interpretation
1,2	Microfluidic chip	2-250 nL	Optical microscopy	Poisson process
3		0.1-1,000 μ L		
4,5	Microfluidic chip	2-150 nL	Light microscopy	Poisson process
6	Microfluidic chip	5 μ L	Optical microscopy	Poisson process
7				
8	LQELT	10-20 nL	Light-polarisation	Stochastic process
9			Voltage Measurements	Poisson process
10	Crystallisation platform	1.5 mL	Transmittivity	Poisson process
11	Various reactors	10-1000 mL		Poisson process
12	Crystallisation platform	10-1000 mL		Poisson process
13,14	Crystallisation platform	6 mL	Optical microscopy	Stochastic process
15	Various reactors	15-150-500 mL	Direct observation	Stochastic process
16	Crystallisation platform	5 mL		Poisson process
17		15 mL		Stochastic process
18		30 mL		Poisson process
19	Crystallisation platform	1-2 mL	Transmittivity	Poisson process
20	Various reactors	1.8-250-1,000 mL	Turbidity	Stochastic process

$1/(JV)$. This shows that not only the average nucleation time, but also the standard deviation – hence the expected variability in measurements of nucleation times – decrease with volume.

From this interpretation a seemingly reassuring picture seems to emerge: the stochastic nature of nucleation fades away as V increases, and the variability in measured nucleation times vanishes accordingly. It is also worth noting that in the frame of a deterministic description of nucleation, where JV gives the deterministic rate of formation of new crystals per unit time in the volume V , the nucleation time, t_n , can be predicted as the time when the first nucleus is deterministically formed. This is the time at which the following integral, which gives the number of crystals that have formed, equals 1:

$$\int_0^{t_n} J(t)V(t)dt = 1 \quad (4)$$

At constant nucleation rate and volume, $t_n = 1/(JV)$, i.e. the nucleation time in the deterministic interpretation of nucleation equals the average nucleation time of Eq. (1) in the stochastic description (at constant supersaturation and volume). The crucial difference is of course that in the former interpretation all nucleation experiments are perfectly reproducible at any scale, whereas in the latter description nucleation times hence experimental outcomes are distributed, their degree of variability decreasing monotonically with increasing system volume.

It is worth noting that a stochastic behaviour in smaller volumes and a deterministic behaviour in larger volumes are consistent with the mononuclear mechanism and the polynuclear mechanism, respectively, used by Kashchiev, Verdoes and van Rosmalen to describe nucleation and to derive expressions for the experimental induction time in their seminal paper¹.

Unfortunately, there are several pieces of evidence that urge us to challenge the picture of nucleation above.

First, experimental evidence indicates that also in large vessels, i.e. where the standard deviation of nucleation times should be so small to be effectively negligible, nucleation is poorly reproducible^{2,3}.

Secondly, the description of nucleation as a Poisson process is correct only if the evolution of the system at any time does not depend on previous stochastic events. This is true only for the formation of the first nucleus, but not for the next ones, particularly when the further growth of nuclei that were previously formed contributes to the depletion of supersaturation.

Finally, the nucleation time is in general not observable. What one can measure is the detection time t_d , which – though differently defined depending on the system and the measurement apparatus – is typically the time when a certain fraction of the solution volume is occupied by the newly formed crystals. In this case, one needs information about crystal growth rate in order to interpret quantitatively the outcome of the experiments. Alternatively, and typically in microfluidics, one uses optical microscopy to look at many micro-crystallisers and to measure in how many of them at least one particle was formed. Both types of information can be used to build a statistics, but they present different challenges when one wants to interpret the data quantitatively using a model.

Though in many ways successful from an experimental or a theoretical perspective, the papers listed in Table 1 are not yet answering a question of key

importance. Can the nucleation kinetics estimated in small volumes be used to describe nucleation when scaling up the process? Although we are fully aware that when scaling up many features of the crystalliser and of the process can lead to deviations and differences, we do believe that there might be more than that to justify the difficulties experienced and reported in the literature, e.g. in a recent study carried out by a group at the Technical University of Delft (TU Delft). We believe that there is a need to find ways to account for the stochastic behaviour observed at smaller scale in the description of nucleation at larger scale, and this is indeed the objective of this paper. First, we will summarise the results reported earlier that will be used as backbone and benchmark of our analysis. Then, we will use two different models to describe those data; a first model, which though similar to what the TU Delft group proposed seems to us to be physically more consistent, and a second one, which to the best of our knowledge is novel and attempts to incorporate stochasticity also in the description of nucleation processes where a large number of crystals are formed, in an arbitrary large volume and non-constant temperature. Finally, we will discuss our findings and draw conclusions.

2 Background

2.1 Literature review

The relevant literature for this work, i.e. concerning stochastic effects in nucleation, is summarised in Table 1, where for each paper the system volume used, the detection technique applied and the interpretation of the experiments provided are reported.

Detection techniques can be divided into two main categories. The first relies on direct observation of crystals *via* optical microscopy, where the detection of crystals depends on the resolution of the optical instrument^{4–14}. In the second category, fall the experiments where a macroscopic system property (such as transmittivity or turbidity), which is related to the volume fraction of the crystals, is measured^{2,15–24}. Crystals are detected, hence the detection time is measured, when such volume fraction exceeds a specific threshold value. This latter technique suffers from two weaknesses: first, the quantitative relationship between solid volume fraction and for instance turbidity is difficult to calibrate; secondly, the threshold value is extremely difficult to estimate and might well be dependent on a series of factors, e.g. instrument sensitivity, system intrinsic properties, fluid-dynamic effects. Observation using optical microscopy is typically utilized in very small volumes, whereas macroscopic measurements are exploited in larger volumes.

The time associated to the observation of crystals in the system, obtained either by direct observation or by indirect measurements, can be used to quantify nucleation kinetics. To this purpose, a physical and mathematical model of the entire crystallisation process must be provided. Such model needs to account, on the one hand, for the stochastic nature of nucleation itself, e.g. assigning a statistics to describe the distribution of experimental data, and, on the other hand, for the combined action of nuclei formation, which is stochastic, and growth until detection, which is deterministic.

Assumptions concerning the growth process are hence necessary to interpret the experimental data. In microscopic systems, it is often possible to assume that growth is much faster than nucleation, so that the time between particles formation and detection is negligible, i.e. $t_n \approx t_d^{9-14}$. Alternatively, still in microscopic volumes, one can decouple nucleation and growth and analyse them independently, as for example by applying the so-called double-pulse technique⁴⁻⁸.

An example of a microfluidic study where an optical technique has been used is the work of the group at the University of Illinois at Urbana-Champaign that performed isothermal experiments on the crystallisation of paracetamol and lysozyme from evaporating aqueous micro-droplets¹¹. Assuming that growth is infinitely fast hence that the statistics of Eq. (1) can be directly applied to detection times, they could estimate the parameters of the following classical nucleation rate expression:

$$J(S) = q_1 S c^* \exp\left(-\frac{q_2}{\ln^2 S}\right) \quad (5)$$

where c^* is the solubility at the experimental temperature, $S = c/c^*$ is the supersaturation, and q_1 and q_2 are constant parameters. They could show that the estimated nucleation rate exhibited good predictive capabilities when changing operating conditions (but not the droplets' volume).

2.2 TU Delft study

The study carried out by a group at the TU Delft will be used in the following as a benchmark². They carried out a large number of experiments of cooling crystallisation of paracetamol from aqueous solutions in vessels of different volumes. In particular, in a 1 mL crystalliser they explored four different initial paracetamol concentrations, always starting the linear cooling process from the corresponding saturation temperature. Then, they carried out systematic experiments also in larger crystallisers, namely of volumes of 500, 700, 900 and 1,000 mL. In each experiment the detection time was measured, and cumulative distribution curves of detection times were obtained at each initial concentration and for each crystalliser volume. The two sets of data at the lowest and highest concentration explored, namely 15 g/L and 47 g/L (the others being 22 g/L and 32 g/L) are reported in Figure 1, where the cumulative probability is plotted as a function of the temperature change between time zero and the detection time, ΔT . It can be observed that the qualitative behaviour of the cumulative probability curves is in accordance to equation (2) and (3), i.e. the average value of ΔT , hence of the detection time, and the standard deviation decrease with increasing volume.

The data at 1 mL were then used to estimate the parameters of the model that was finally applied to predict the data measured in larger volumes. The model assumed that nucleation occurred through a mononuclear mechanism and was followed by growth of the single crystal to a threshold size r_a , where it was finally shattered by attrition, causing a burst of secondary crystals, which were immediately detected. Therefore the detection time, t_d , is the sum of the nucleation time, t_n , and of the deterministic growth time, t_g . The latter is equal to the ratio between the threshold size r_a and a growth rate, G , which is assumed to be the same for all the experiments at a given initial concentration. The nucleation

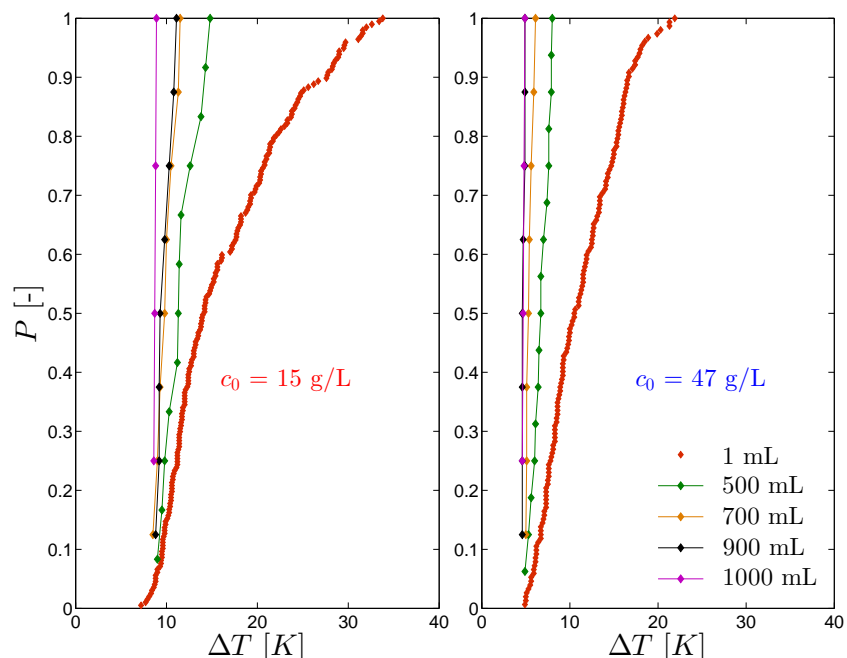


Fig. 1 The TU Delft experimental data of detection times, expressed as cumulative nucleation probability, P , vs the extent of cooling, ΔT , for the cooling crystallisation of paracetamol from aqueous solution². The experiments shown here represent two different initial concentrations, 15 g/L (left) and 47 g/L (right), for crystallisers of five different volumes. The lines connecting the data at larger volumes (from 500 to 1000 mL) are drawn as guide for the eye.

time t_n , on the other hand, is assumed to be distributed according to the Poisson distribution of Eq. (1), with $k(t) = VJ(t)$; the nucleation rate depends on time due to cooling and is given by the following expression:

$$J = a \exp\left(-\frac{b}{\ln^2 S}\right) \quad (6)$$

where a and b are in principle temperature dependent, but are assumed to be constant for each initial concentration level, but different for the different initial concentrations. The TU Delft group related the threshold size to a growth time, t_g by: $t_g = r_a/G$, with $G = k_g(S - 1)$, the crystal growth rate. After determining the threshold size through experiments, they estimated the three parameters k_g , a , and b for each of the four sets of 1 mL experiments, thus obtaining twelve parameters in all (see Tables 1 and 2 in the original paper²).

Although the agreement between model results and experiments is quite satisfactory, there are a number of issues. First, assuming temperature independent rates of nucleation and growth is clearly inconsistent with the experimental evidence, where metastable zone widths between 20 and 30 K are observed. Secondly, using different sets of parameters for different initial concentrations and temperatures allows for a rather empiric account of temperature effects, which makes it impossible to expect that the model parameters can be used in

a predictive manner, e.g. to describe the effect of different initial concentrations or different cooling rates. Finally, there is no quantitative agreement with the measurements in the larger crystallisers ($V = 500, 700, 900$ and $1,000$ mL); as already noted by the authors, the Poisson model predicts a much faster transition to a deterministic behaviour with increasing volume than the one experimentally observed.

The difference between the model based on 1 mL experiments and the measurements in larger volumes can be due to different reasons. For example, the mixing in the vessel might not be good enough to assure that the desired temperature profile is reproduced at all the tested scales. It could also be possible that hot or cold spots form locally in the larger crystallisers, thus locally altering the nucleation rate. Another explanation can be that, by changing the reactor, a different surface is provided to the system, maybe changing the nucleation mechanism. Moreover, the different batches might have been influenced by a different presence of dust or other impurities, hence preventing the possibility of a straightforward scaling. Finally, the detection limit determined in small volumes might not be appropriate in larger volumes. This was explicitly discussed in the frame of the theory of nucleation based on the mononuclear and polynuclear mechanism², but not considered in the work of the TU Delft group.

3 Modelling stochastic nucleation in crystallisation

Our goal is to analyse different approaches to modelling crystallisation processes at different scales while accounting for stochastic nucleation. We will try and improve on the TU Delft approach, and use their experimental data as a case study and for benchmarking. More specifically, we will present and discuss two different models that differ in how nucleation is described but are based on the common assumptions that are discussed in the following.

We describe a crystallising system of constant volume V undergoing batch cooling crystallisation, starting from an initial temperature T_0 where the solution is saturated and clear. During the cooling, an arbitrary number N of particles can form. The size of the particles, having a single characteristic dimension L , is distributed according to the 1D-particle size distribution (PSD) $f(t, L)$; the quantity $f(t, L)dL$ is the concentration of particles of size between L and $L + dL$; the j^{th} -order moment of the PSD, $\phi_j(t)$, is defined as:

$$\phi_j(t) = \int_0^\infty L^j f(t, L) dL \quad (7)$$

The linear cooling process is characterized by the following relationship:

$$T(t) = T_0 - \beta t \quad (8)$$

where the cooling rate β [K min^{-1}] is constant; note that the initial solute concentration c_0 equals the solubility at the initial temperature, i.e. $c^*(T_0)$.

The zero-th order moment of the PSD, $\phi_0(t)$, is the number of particles per unit volume, hence

$$N(t) = V\phi_0(t) \quad (9)$$

The third order moment of the PSD, $\phi_3(t)$ multiplied by k_v , represents the volume fraction of solids in the suspension; through the mass balance it is linked to the solute concentration $c(t)$ and to its initial concentration, c_0 :

$$c_0 = c^*(T_0) = c(t) + k_v \rho_c \phi_3(t) \quad (10)$$

where ρ_c is the crystal density [kg m^{-3}], and k_v the shape factor. In agreement with the literature^{2,3}, the detection time t_d is the time when $k_v \phi_3(t)$ reaches a threshold value α , i.e.:

$$\frac{V_c(t_d)}{V} = k_v \phi_3(t_d) = \alpha \quad (11)$$

In the following we will always use the same value for such threshold, namely $\alpha = 10^{-4}$.

Table 2 The coefficients and the physical parameters used in the present work.

Parameter	Value
β [K min^{-1}]	0.5
ρ_c [kg m^{-3}]	1260
k_v [-]	$\pi/6$
Γ_0 [g L^{-1}]	7.147
Γ_1 [$\text{g L}^{-1} \text{K}^{-1}$]	$1.986 \cdot 10^{-1}$
Γ_2 [$\text{g L}^{-1} \text{K}^{-2}$]	$5.048 \cdot 10^{-3}$
Γ_3 [$\text{g L}^{-1} \text{K}^{-3}$]	$-1.273 \cdot 10^{-4}$
Γ_4 [$\text{g L}^{-1} \text{K}^{-4}$]	$3.0188 \cdot 10^{-6}$

In this work, as an exemplification but without loss of generality, we use the nucleation rate, J , and the growth rate, G , based on the classical nucleation theory and on the (size independent) birth and spread growth model, respectively^{3,25}. They are expressed in such a way that their temperature dependence is explicitly accounted for:

$$J(S, T) = A_0 S \exp\left(-\frac{A_1}{T}\right) \exp\left(-\frac{B}{T^3 \ln^2 S}\right) \quad (12)$$

$$G(S, T) = K_0 \exp\left(-\frac{K_1}{T}\right) (S-1)^{2/3} (\ln S)^{1/6} \exp\left(-\frac{K_2}{T^2 \ln S}\right) \quad (13)$$

Both rates depend on three independent parameters each, namely A_0 , A_1 and B for the nucleation rate, and K_0 , K_1 and K_2 for the growth rate, and on the supersaturation, defined as $S = c/c^*(T)$, using an empirical temperature dependent solubility, namely that of paracetamol in water, which is given by the following polynomial expression²⁶:

$$c^*(T) = \sum_{i=0}^4 \Gamma_i (T - 273.15)^i \quad (14)$$

The parameters Γ_i have been fitted on experimental data from the literature².

3.1 Model 1: stochastic onset of nucleation

In Model 1, we assume that the first nucleation event, i.e. the formation of the first nucleus, occurs as a Poisson process, i.e. following the statistics of Eq. (1), and triggers the start of a deterministic process, through which new nuclei are formed while existing ones grow; the deterministic part of the process can be modelled using a deterministic population balance equation (PBE). Additionally, we assume perfect mixing, no secondary nucleation, no agglomeration and no breakage. Such model is consistent with the mononuclear nucleation mechanism, whereby in small volumes and for slowly nucleating substances, the appearance of the first nucleus triggers a change of regime, i.e. a transition from a metastable state to a deterministic evolution¹. It bears also an obvious similarity to the simplified model proposed by the TU Delft group and summarised in section 2.2².

The process is described as follows. The cooling crystallisation process starts at $t = 0$, with the temperature following the linear cooling profile of Eq. (8) and the solute concentration constant at $c = c_0$; no crystals are present. At time t_n the first nucleus appears; since nucleation is assumed to be a non-homogeneous Poisson process, the statistics of t_n follow Eq. (1), given in the form:

$$P(t_n) = 1 - \exp\left(-V \int_0^{t_n} J(t') dt'\right) \quad (15)$$

with J given by Eq. (12). After time t_n , the system evolves in a deterministic manner following the equations reported below, whose initial conditions are assigned at $t = t_n$. Note that in term of PSD, and its moments, at t_n only one crystal of negligible size is present.

To describe the evolution of the crystals from t_n on, we use a 1D-PBE or, alternatively but equivalently, the associated *Equations of Moments* (MoM equations)^{27,28}. The standard 1D-PBE for a batch crystalliser where growth is size independent is:

$$\frac{\partial f}{\partial t} + G \frac{\partial f}{\partial L} = 0 \quad (16)$$

with G calculated through Eq. (13), and initial and boundary conditions given by:

$$\begin{aligned} f(t = t_n, L) &= \frac{\delta(t - t_n, L)}{V} \\ f(t, L = 0) &= \frac{J}{G} \end{aligned} \quad (17)$$

The corresponding MoM equations are:

$$\frac{d\phi_j}{dt} = J\delta_{j0} + jG\phi_{j-1} \quad j = 0, 1, 2, \dots \quad (18)$$

where δ_{j0} is the Kronecker symbol and $\phi_{-1}(t) = 0$; the initial conditions are:

$$\begin{aligned} \phi_0(t_n) &= \frac{1}{V} \\ \phi_j(t_n) &= 0 \quad j > 0 \end{aligned} \quad (19)$$

Since here we are interested only in computing the values of t_d according to Eq. (11) and in some average properties, we solve the MoM equations (18) for $j = 0, 1, 2, 3$.

It is rather clear that this model, which might be realistic in a very small volume of solution, loses credibility when the suspension volume increases. It is in fact counter-intuitive that the formation of a critical nucleus in a specific position in the solution volume impacts immediately the course of nucleation in the whole volume and renders the formation of further nuclei fully deterministic. Therefore, the sharp separation between a stochastic nucleation mechanism for the first crystal and a deterministic growth mechanism (as assumed here and in the TU Delft model) seems to be unphysical; this observation motivates us to pursue an alternative description where stochasticity and determinism coexist at least during the early stages of the crystallisation process.

3.2 Model 2: stochastic primary nucleation

In the case of Model 2, we assume that all nuclei, not only the first one as in Model 1, are formed stochastically. After formation, each nucleus grows independently and deterministically, thus giving its deterministic contribution to the depletion of the supersaturation in solution. In such a framework, the time when older nuclei were stochastically born influences the conditions at which future nuclei are stochastically born.

Such effect of the past on the future leads to a new type of stochastic process, namely the so called *self-exciting point process*²⁹, which can be viewed as a generalization of a non-homogeneous Poisson process (see Eq. (1)) where the function $k(t)$ is stochastic, as it depends on a sequence of past stochastic events. In the case of self-exciting point processes in fact, the distribution of the time intervals between two subsequent nucleation events is the same as in a Poisson process, but the relevant value of $k(t)$ is not only time-dependent but also stochastic. In other words $k(t)$ depends on *more* than time t only. Therefore the self-exciting point process can be understood as a step-by-step non-homogeneous Poisson process. Therefore the probability, P_1 , that at least one new nucleus forms in the time interval $\Delta t = t_i - t_{i-1}$ is the complement to one of the probability that in the same time interval no new nuclei form, P_0 ; one can thus write:

$$P_1(t_{i-1}; t_i) = 1 - P_0(t_{i-1}; t_i) = 1 - \exp\left(-V \int_{t_{i-1}}^{t_i} J(t') dt'\right) \quad (20)$$

where the time dependence of the nucleation rate, J , is affected by the formation of nuclei in the previous time interval from 0 to $t = t_i$.

Each new crystal, which is born at $t = t_{n,k}$ and is labelled k ($\forall k = 1, 2, \dots$), grows independently according to the following deterministic equation:

$$\begin{aligned} L_k &= 0 & t &\leq t_{n,k} \\ \frac{dL_k}{dt} &= G(S, T) & t &> t_{n,k} \end{aligned} \quad (21)$$

The population of crystals is in this case discrete and the crystal volume fraction,

which is proportional to its third moment, is given by:

$$\frac{V_c(t)}{V} = k_v \phi_3(t) = \frac{k_v \sum_{j=1}^{N(t)} L_j^3(t)}{V} \quad (22)$$

with $N(t)$, the number of crystals at time t . With this definition, the mass balance of Eq. (10), and the detection condition, Eq. (11), can be computed. Note that $N(t)$ is a monotonically increasing staircase function, with $N(0) = 0$ and all the step increments equal to 1.

Modelling primary nucleation as a self-exciting point process has two important consequences. First, from a physical point of view, the self-exciting point process of Model 2 applied to the formation of all crystals in the system should exhibit a higher degree of variability than the Poisson process of Model 1, which applies only to the first nucleus. This is a straightforward consequence of the coexistence of stochastic and deterministic mechanisms during the formation and the growth of all the particles in suspension. It should nevertheless be noticed that, in line with experimental evidence, the overall variability still reduces with increasing volume since the probability of particle formation is governed by Eq. (20) where the volume appears in the exponent and with a negative sign.

The second consequence is of numerical nature: the self-exciting processes can be simulated exactly when their intensity rate $k(t)$ is known, as in our case, by applying an inversion algorithm. Starting from the initial condition, $N_0 = 0$, we generate a uniformly distributed random number and find the time corresponding to it drawn from the exponential distribution given in (20), i.e., we compute the time interval Δt elapsing before the first nucleation event occurs, ($\Delta t = t_{n,1} - 0$). We afterwards update the system, which now counts one particle and compute the new time interval for the nucleation of the second particle, $\Delta t = t_{n,2} - t_{n,1}$, this time solving also Eq. (21) and (22) at each time step, while using Eq. (20). The procedure is repeated until the detection condition is met. This simulation technique is fundamentally different from the Monte Carlo algorithm suggested by Biscans et al.¹⁰, based on a rejection method. In a Monte Carlo algorithm the integration step, Δt , determines the number of time the rejection process is called. Too fine or too coarse choices can over- or under-estimate the number of nuclei that form. A large number of simulations is needed simply to validate the correct time step, seriously limiting the applicability of this specific method for regressing nucleation parameters.

4 Results

In this section the results obtained with the two models described above are reported. First, Model 1 is used to regress the experimental data from TU Delft; the quality of the fitting, its predictive capabilities and the correlation among the parameters of the nucleation and growth rate expressions are discussed. Then the obtained parameters are used in Model 2; similarities and differences between the two models are analysed, and simulation illustrating the effect of changing cooling rate is reported and discussed. Since the focus is on stochastic nucleation and scaling from small to large volumes, all results will be presented so as the reader is informed not only about average properties of the crystallisation process but also about their statistic distribution.

4.1 Model 1: parameters' estimation

Model 1 has been applied to estimate the six parameters in the nucleation and growth rate expressions of Eqs. (12) and (13) by fitting the experimental detection times measured by the TU Delft group in the 1 mL crystalliser at two different initial concentrations, namely 15 and 47 g/L, with the calculated ones. The values of the six estimated parameters are reported as *Reference kinetics* in the second column of Table 3. Figure 2 shows the experimental cumulative distributions of detection times, the corresponding calculated distributions, as well as the calculated distributions of nucleation times.

Table 3 Kinetic parameters obtained from fitting the 1 mL-crystalliser data of TU Delft².

Parameter	Reference kinetics	Faster growth	Slower growth
A_0 [$\text{m}^{-3} \text{s}^{-1}$]	7.55×10^3	8.410×10^3	5.5×10^3
A_1 [K]	660	570	630
B [K^3]	7.35×10^5	2.15×10^6	1.3×10^5
K_0 [m s^{-1}]	1.67×10^{-4}	1.67×10^{-3}	8.35×10^{-5}
K_1 [K]	1.0×10^3	1.0×10^3	1.0×10^3
K_2 [K^2]	3.22×10^3	3.22×10^3	3.22×10^3

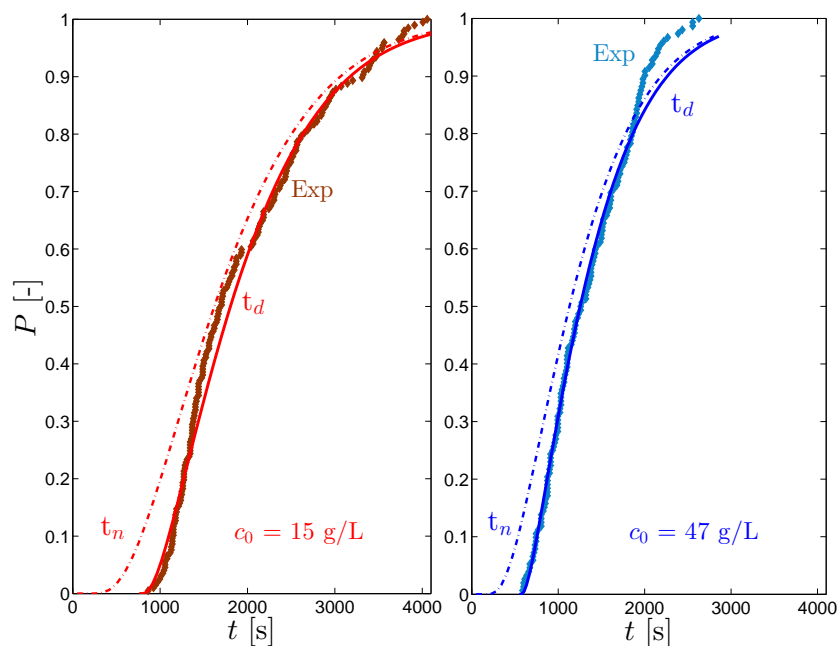


Fig. 2 Results of Model 1 and experimental data of TU Delft² in 1 mL vessel. Symbols: experimental data; solid lines: detection time probability curves; dashed lines: nucleation time probability curves (given by Eq. (1)).

A few remarks are worth making. The model predicts a detection time, which is between 0 s and about 400 s larger than the nucleation time. This indicates the importance of growth in these crystallisation experiments on paracetamol from aqueous solution. It is also worth noting that due to cooling, the later the nucleation, the lower the temperature and the higher the supersaturation at which it occurs; higher supersaturation (that speeds growth up) prevails on lower temperature (that slows it down), thus leading to a decrease in growth times for larger values of t_n (from about 400 s, when nucleation is the fastest, to essentially 0 s, i.e. instantaneous growth to the detection size, when $t_n \approx 4,000$ s).

The agreement between measured and simulated detection times is rather good, not only at the initial concentrations of 15 g/L and 47 g/L, but also at 22 g/L and at 32 g/L (data not shown here). This is an important result, because such a good fitting has been obtained with temperature dependent rate models for nucleation and growth, where only six parameters have been estimated. The resulting model can reliably be used to predict crystallisation at different initial concentrations and for different cooling rates, i.e. something not possible with the TU Delft model and their twelve estimated parameters.

When looking more in detail, at $c_0 = 47$ g/L a deviation between experiments and simulations can be observed at values of the detection time beyond about 1,800 s. In fact the experimental data for $t_d > 1,800$ s seem to follow a different trend with respect to those for $t_d < 1,800$ s. Considering that upon cooling supersaturation increases, a change of nucleation mechanism might explain the deviation, particularly considering that the supersaturation is as high as 1.8 when nucleation leading to $t_d = 1,800$ s occurs. However more experimental data would be needed to demonstrate this property thoroughly.

4.2 Model 1: effect of volume

Figure 3 illustrates results for larger crystalliser volumes, namely 500, 700, 900, and 1,000 mL; each diagram refers to a specific volume as indicated, and shows the experimental cumulative distributions of detection times (for the two initial concentrations, namely 15 g/L and 47 g/L associated to larger and smaller detection times, respectively), and the corresponding distributions of both detection times and nucleation times calculated using Model 1 with the *Reference kinetics* parameters.

It is rather clear that the model is in general not able to describe the experiments, as it happens in the case of the model developed by the TU Delft group². The model is unable to consistently predict the average detection times, and underestimates their variability; The experiments exhibit a much larger variability than predicted by the model. This behaviour might be due to a model mismatch that makes the extrapolation to larger volumes infeasible, or to the same reasons spelled out above with reference to the attempts made by the TU Delft group (see section 2.2). We also tried to specifically fit the measurements in larger volumes with a set of *ad hoc* parameters different from the *Reference kinetics* in Table 3, without achieving satisfactory results though.

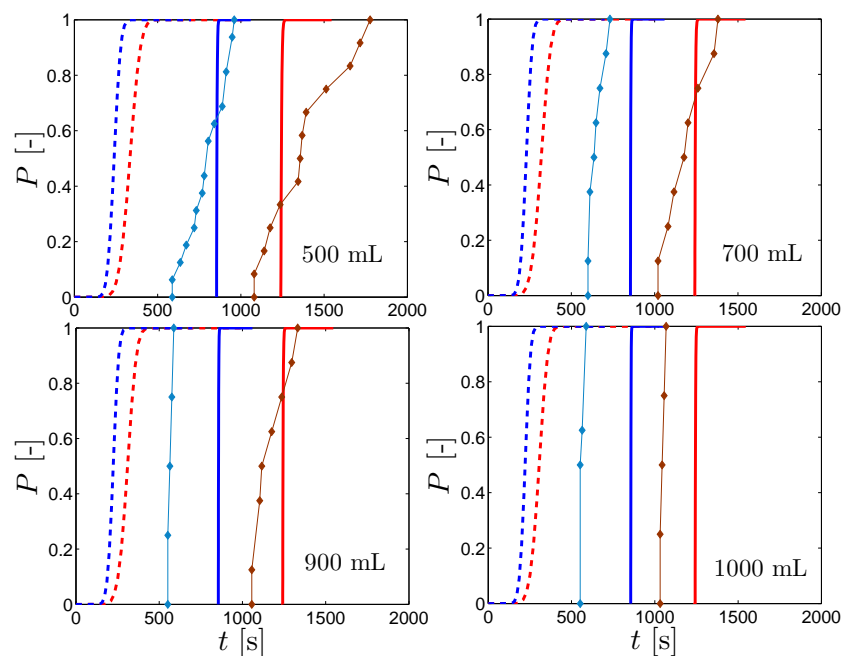


Fig. 3 Results of Model 1 and experimental data of TU Delft², in 4 different volumes. Initial concentrations are 15 (red) and 47 (blue) g/L. Symbols: experimental data; solid lines: detection time probability curves; dashed lines: nucleation time probability curves (given by Eq. (1)).

4.3 Model 1: correlation among parameters

The set of parameters indicated as *Reference kinetics* in Table 3 have been obtained by minimizing the deviation between experiments and simulations using a standard optimizer. By analysing the results, one realizes that the objective function for this problem is rather flat, and the minimum rather shallow. In fact, the estimated model parameters are correlated; in other words, very similar distributions of detection times as the one plotted in Figure 2 can be obtained by increasing the growth rate and reducing the nucleation rate, or vice versa.

To demonstrate this, we have selected two different sets of values for the growth rate parameters, and estimate the nucleation rate parameters to minimize the error between experiments and simulations. As reported in Table 3, the growth rate constant K_0 has been set to a value ten times larger (column 3, *Faster growth*) and to a value two times smaller (column 4, *Slower growth*) than that of the *Reference kinetics*, whereas K_1 and K_2 have been kept unchanged. After fitting, the nucleation rate parameters A_0 , A_1 and B have attained the new values also reported in Table 3.

Figure 4 illustrates the results, by showing the experimental detection time distributions at the two concentrations considered in the 1 mL crystalliser, together with the same distributions calculated with the three different sets of parameters; it is rather clear that the fitting accuracy is quite comparable. In the insets, the distributions of nucleation times for the two initial concentration levels (on

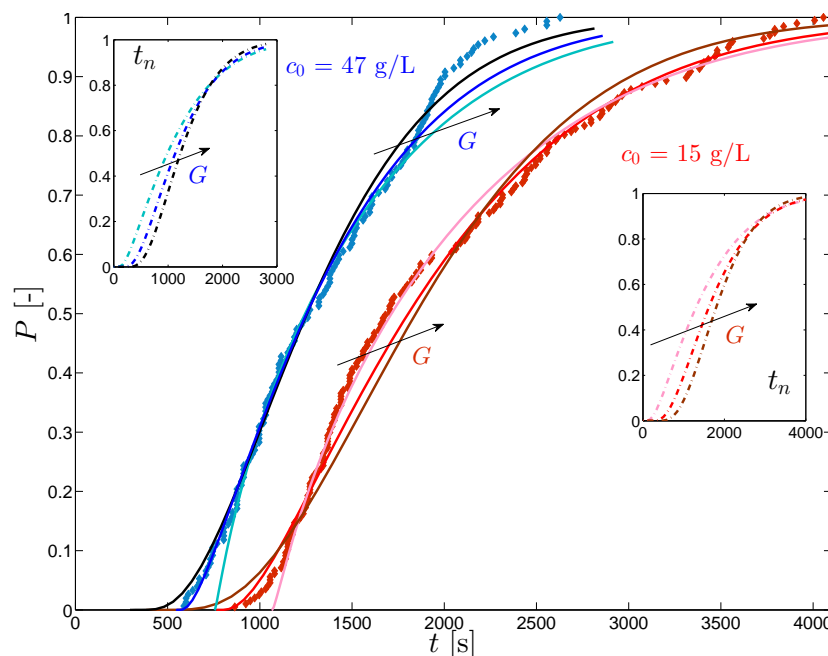


Fig. 4 Results of Model 1 with three different sets of kinetic parameters (cfr. Table 3) and experimental data of TU Delft² in 1 mL. In the main figure, symbols: experimental data; solid lines: detection time probabilities. In the figure insets, dashed lines: nucleation time probability (given by Eq. (1)). For $c_0 = 15$ and 47 g/L (red and blue shades, respectively), G increases from the lightest to the darkest colour.

the l.h.s. and on the r.h.s. the larger and the smaller concentration, respectively), as calculated with the three sets of parameters are also plotted. One can readily observe that indeed nucleation times are the longest for the set of *Faster growth* parameters, whereas the *Reference kinetics* yields intermediate values of t_n .

Thus concluding, estimating nucleation and growth rate parameters from statistics of detection times only is not possible, because the two groups of parameters are highly correlated, which is a mathematical property reflecting the physical reality that both nucleation and growth contribute to determine detection times. To overcome this problem, either independent growth measurements or additional, different pieces of information (e.g. the number of particles or the average particle size at some time t) are required.

Interestingly though, the simulation results indicate that, if in 1 mL the different sets of kinetic parameters yield very similar distributions of detection times, in larger volumes the corresponding distributions are well distinct. This is illustrated in Fig. 5 for the case of $c_0 = 47$ g/L, where the cumulative distributions of nucleation and induction times obtained for the three sets of kinetic parameters are plotted and compared with the experimental distributions. It is worth noting that by and large the *Faster growth* parameters do a better job than the two other sets. Although one might be tempted to argue that the volume effect could be used to identify the best among different sets of parameters, in reality one should be cautious and rule out first the possible causes of differences in measured de-

tection times when scaling up the system volume, as discussed in section 2.2.

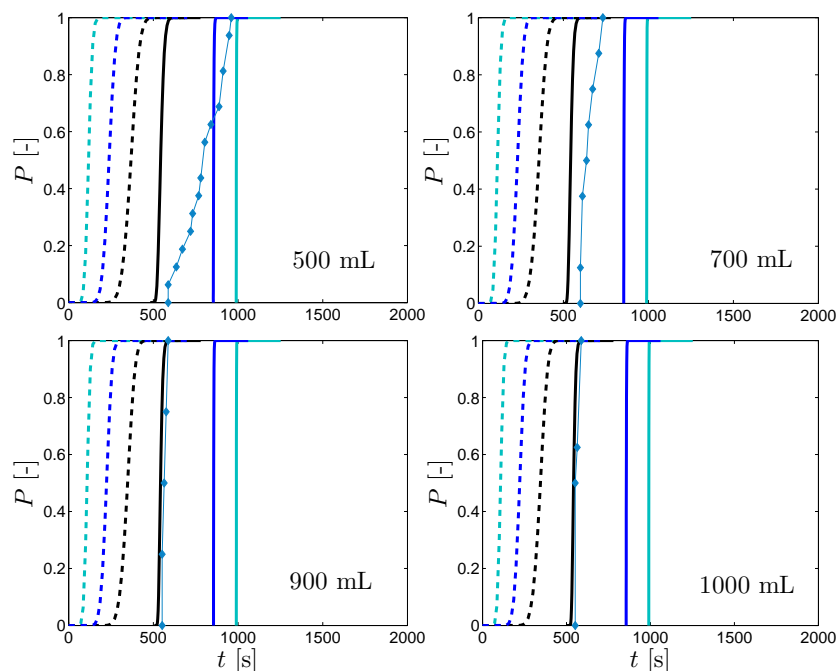


Fig. 5 Results of Model 1 with 3 different sets of kinetic parameters (cfr. Table 3) and experimental data, in 4 different volumes, for $c_0 = 47$ g/L. Symbols: experimental data of TU Delft²; solid lines: detection time probabilities (given by Model 1); dashed lines: nucleation time probability (given by Eq. (1)). G increases with colour from light blue to black.

4.4 Model 2: comparison with Model 1

Let us now consider Model 2; for the sake of comparison with Model 1, rather than estimating a new set of kinetic parameters, we have used the *Reference kinetics* set of parameters in Table 3 and carried out simulations of nucleation and growth with both models, starting from the two reference initial concentration values and for a number of system volumes between 1 mL and 1,000 mL. Each simulation using Model 1 or Model 2 has been performed independently and, for each volume V at each initial concentration c_0 , at least one thousand simulations have been carried out in order to build reliable statistics.

The key differences between the results obtained with the two models can be appreciated by examining Figure 6, which plots the total number of particles present at the detection time, i.e. $N(t_d)$, for simulations carried out at different initial concentration, c_0 , and different system volume, V . Let us focus on the results for $c_0 = 15$ g/L and $V = 100$ mL; similar considerations can be made for all the other cases. There are two sets of points: the aligned brown (darker) symbols on the l.h.s. obtained through Model 1, and the red (lighter) symbols, forming a cloud on the r.h.s. and calculated using Model 2.

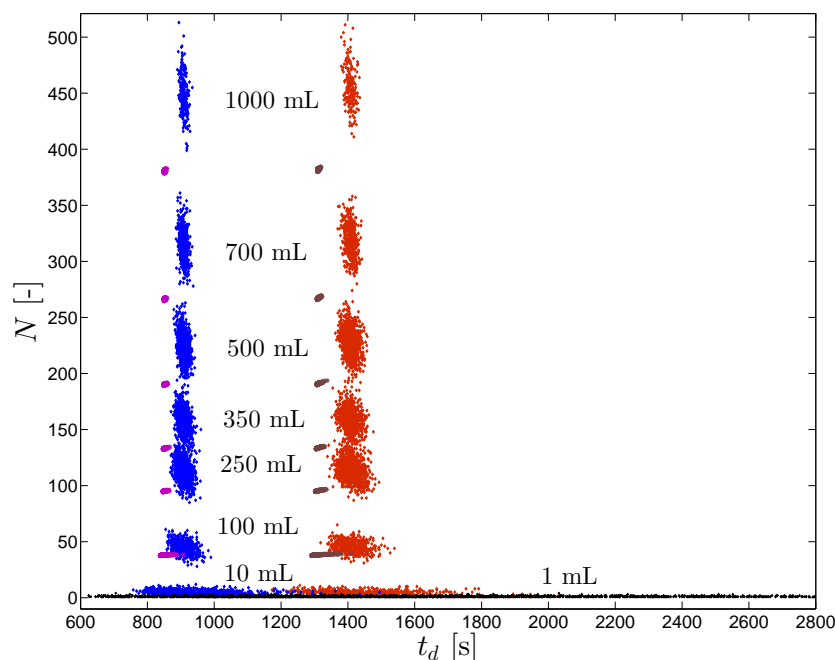


Fig. 6 Results of simulations of Model 2 given as number of crystals, N , formed at the detection time, t_d , for different volumes. Two different initial concentrations, 15 and 47 g/L, are represented in red and blue, respectively, for volumes from 10 to 1000 mL. Results of simulations in 1 mL volume, largely overlapping for both initial concentrations, are all represented in black. Results of simulations of Model 1 for 100, 250, 350, 500, 700, and 1000 mL are indicated as violet and brown points (for $c_0 = 47$ g/L and $c_0 = 15$ g/L, respectively).

In the case of Model 1, the stochasticity of nucleation yields a range of detection times and of number of particles as discussed above; however, for each stochastic value of the nucleation time, there are only one value of the detection time and one number of particles, because after the birth of the first nucleus the evolution of the system is deterministic.

In the case of Model 2 on the contrary, the same detection time may correspond to different numbers of particles, and vice versa; this is indeed the consequence of the co-existence of stochastic nucleation and of deterministic growth after the formation of the first nucleus.

It is also worth observing that, as a consequence of the different structure of the two models, the average detection time and number of particles obtained with Model 2 are larger than those calculated using Model 1. On the one hand, the variability of the detection times decreases with increasing volume for both models, i.e. the self-exciting point process of Model 2 behaves in that respect like the inhomogeneous Poisson process of Model 1. On the other hand, the variability (or the standard deviation) of the Model 2 statistics of detection times is larger than that of Model 1.

Considering the statistics of the number of particles, with increasing volume

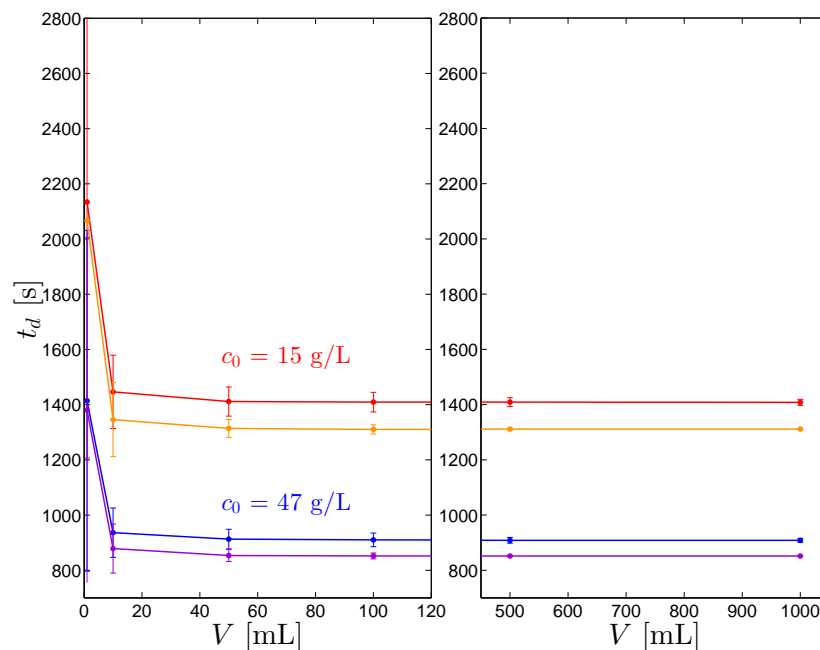


Fig. 7 Results of simulations of Model 2, $c_0 = 47$ 15 g/L (blue), and $c_0 = 15$ g/L (red), and Model 1, $c_0 = 47$ g/L (violet), and $c_0 = 15$ g/L (orange), given as average values of detection times, t_d . In the left figure, the volume ranges from 0 to 120 mL; in the right one, from 450 to 1100 mL. The error bars indicate the standard deviation of the corresponding average t_d value.

the variability of the number of particles calculated with Model 2 increases a lot. It can also be noted that for $V = 1$ mL, i.e. the volume on which the quantitative study of the TU Delft group is based, only a very few number of particles are formed, typically less than five, which correspond to a very broad range of detection times (see Figure 2 for the cumulative probability distribution of the detection times measured and calculated with Model 1 under the same conditions); from $V = 250$ mL on, the number of particles exceeds about one hundred. This result gives a quantitative confirmation and a visual illustration of how at different system volumes a mononuclear or a polynuclear mechanism may be the better way to describe nucleation¹. It shows also that the mononuclear mechanism implicit in the TU Delft model and in our Model 1 is inadequate to describe volumes above 10 mL, in this case.

The same results are illustrated in a different manner for the same two initial concentration values in Figure 7, which shows as a function of the volume, V , the mean detection time, t_d , together with error bars, that are calculated by adding and subtracting from the mean t_d the value of the relevant standard deviation of the t_d distribution. It is worth noting that the two models behave very similarly when $V = 1$ mL, as expected since at that volume a few particles only are formed; since the first nucleus follows the same statistics for both models, with such a small number of particles to be formed, the differences between the results obtained with the two models can only be very small.

4.5 Model 2: sensitivity to kinetic parameters

Simulations using Model 2 have been repeated for the *Faster growth* parameters in Table 3, i.e. the parameters that when using Model 1 exhibited the best accuracy in describing measurements at higher system volumes (see Fig.5). Figure 8 shows as a function of the volume, V , the mean detection time, t_d , together with error bars, calculated as in Figure 7. For each initial concentration value two curves obtained using the two different sets of kinetic parameters are plotted. Moreover, the average detection times observed in the TU Delft experiments in crystallisers with $V = 500$ mL, 700 mL, 900 mL and 1,000 mL are plotted.

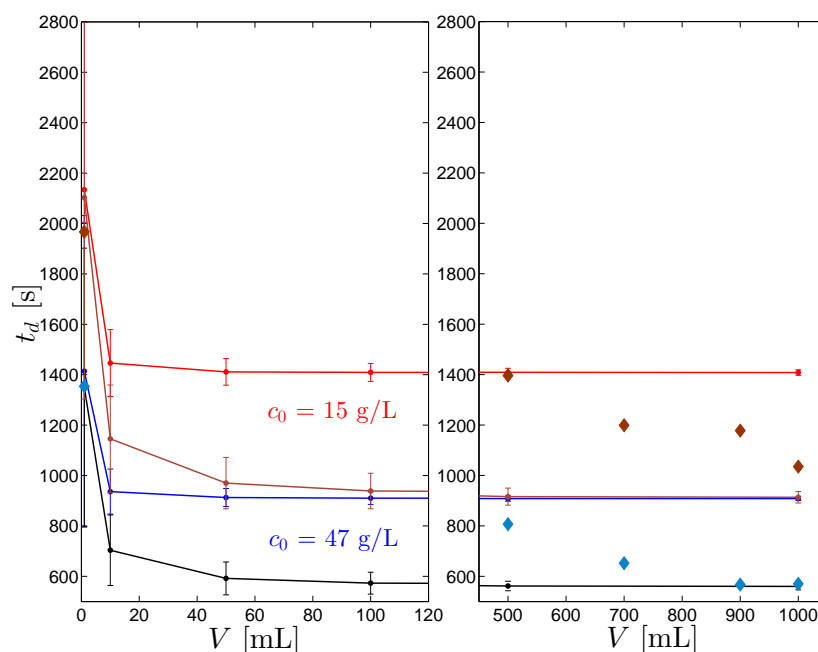


Fig. 8 Comparison of simulations of Model 2, in 1 mL crystalliser, given as average detection times, t_d . Two different sets of parameters, *Reference kinetics* (blue and red, $c_0 = 47$ g/L and $c_0 = 15$ g/L, respectively) and *Faster growth* (black and brown, $c_0 = 47$ g/L and $c_0 = 15$ g/L, respectively) have been used (see Table 3). In the left figure, the volume ranges from 0 to 120 mL; in the right one, from 450 to 1100 mL. The symbols indicate the experimental data of TU Delft² at the corresponding volumes. The error bars indicate the standard deviation of the corresponding average t_d value. The overlapping of the brown and blue line observed here is a coincidence of this particular system, and does not represent a specific feature of the model.

As already observed using Model 1, the two sets of parameters yield very similar results when $V = 1$ mL, but diverge progressively as the volume increases. At both concentrations the *Faster growth* parameters yield lower values of the average detection time (about 500 s less and 300 s less at 15 g/L and at 47 g/L, respectively) and larger values of the standard deviation (which is typical for slower nucleation rates, as discussed in the Introduction when summarizing the main features of a homogeneous Poisson process) than the *Reference kinetics*

parameters.

When comparing in Figure 8 the simulation results and the experimental data, one notices that the experimental data fall in the region delimited by the two curves calculated with the *Reference kinetics* and with the *Faster growth* parameters; the former set works better in the 500 mL crystalliser, whereas the latter in the 900 mL and 1,000 mL crystallisers. Even though the standard deviation calculated with Model 2 is larger than that predicted by Model 1, it is still much smaller than the experimental one.

Thus concluding, though Model 2 is a clear improvement with respect to Model 1 in terms of physical consistency, based on the TU Delft experimental results in large crystallisers only it is not possible to demonstrate that Model 2 is able to capture completely the effects due to the change from very small, microfluidic volumes, to larger ones. It is clear that to this aim more experiments, following a well designed experimental protocol will have to be performed.

4.6 Effect of cooling rate

Being intrinsically temperature dependent, both Model 1 and Model 2 can be used to study the effect of the cooling rate on the crystallisation process, on the nucleation stochasticity, and on the metastable zone width (MZW), i.e. the region of the phase diagram where the solution is supersaturated but nucleation is kinetically hindered.

We have investigated such effect using Model 2 and illustrated it in Figure 9, where the average difference between the temperature at time zero and at the detection time, $\Delta T(t_d)$, i.e. the observed MZW, with its variability (error bars) is plotted vs. the system volume. These have been calculated using the parameters corresponding to the *Reference kinetics* for the initial concentration of 47 g/L and three different cooling rates, namely $\beta = 0.25$ K/min, 0.5 K/min (the value used in all simulations reported so far), and 1 K/min; therefore, the data corresponding to $\beta = 0.5$ K/min have already been reported in terms of average detection time both in Figure 7 and in Figure 8. Such average detection times at large volumes are reported also in Figure 9 beside the corresponding $\Delta T(t_d)$ vs. V curve.

As expected based on physical intuition, larger cooling rates lead to larger values of the MZW (and of its variability) and correspondingly smaller values of the detection time. This is due to the fact that the MZW is determined by the competition between a supersaturation generating mechanism, i.e. cooling, and a supersaturation depleting process, namely particle formation and growth. Changing the cooling rate affects the former but not the latter, thus yielding larger values of MZW, the reduction of the detection time being a mere consequence of the fact that the same temperature change requires less time when the cooling rate is larger.

Our time-dependent model is also able to describe the effect of the stochastic nature of nucleation on the MZW in very small volumes, namely that the MZW and its variability are larger in very small volumes than in large volumes. In volumes beyond a system specific threshold value the MZW reaches an asymptotic value for each cooling rate, and in principle its variability vanishes.

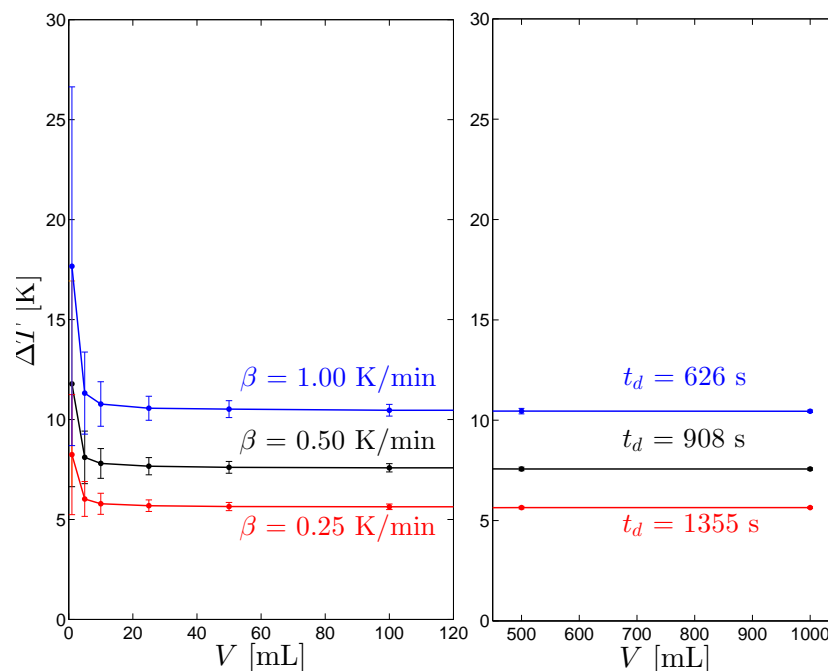


Fig. 9 Results of simulations of Model 2, at different volumes, for $c_0 = 47$ g/L, with three different cooling rates, β , reported as average Metastable Zone Width, $\Delta T'$. In the right-hand-side box, at larger volumes, the asymptotic values of the average t_d for each cooling rate are indicated. In the left figure, the volume ranges from 0 to 120 mL; in the right one, from 450 to 1100 mL. The error bars indicate the standard deviation of the corresponding average $\Delta T'$ value.

5 Discussion and conclusions

This contribution focuses on studying the variability of detection times observed in cooling crystallisation experiments. Such variability has been assumed to be primarily the consequence of an intrinsic stochastic nature of nuclei formation: nucleation is thus mathematically defined as a stochastic process.

Based particularly on the data of paracetamol crystallisation in water, measured by the TU Delft group² in small, well-mixed 1 mL reactors, we have developed two different models (Section 3.1 and 3.2) combining the statistical formation of primary nuclei with their deterministic growth to fully-grown, detectable crystals. Both models not only account for dynamic profiles of temperature and concentration, but they also can be easily modified to describe system with a non-constant volume. Consequently, they can be used directly to analyse isothermal as well as non-isothermal nucleation experiments, and crystallisation where the driving force is not due to cooling, but, e.g., solvent evaporation or anti-solvent addition.

Model 1 (Section 3.1) assumes that the stochastic nature of nucleation, modelled as a Poisson process, influences only the very beginning of the crystallisation, i.e. the formation of the first particle, whereas the subsequent nuclei form-

ation is perfectly deterministic and described by a Population Balance Equation or, equivalently, by the method of moments. The effect of nucleation stochasticity determines only the time *when* the system shifts to the deterministic regime. Model 2 (3.2), on the contrary, considers that the formation of all nuclei, not only the first one, is stochastic, whereas their growth is deterministic.

As suggested by physical considerations and experimental evidence, the magnitude of detection time variance reduces with increasing system volume in both models. However, due to the different stochastic process used to describe nucleation, the second model exhibits always a larger detection time variability.

Model 1 has been used for regressing nucleation and growth kinetic parameters, whose correlation has also been investigated. We concluded that a unique set of parameters cannot be obtained from one series of experiments, if only information concerning the detection times in one single volume is provided. Under these conditions, independent growth measurements are necessary to avoid parameters correlation. Nevertheless, both models show that different sets of kinetic parameters, which yield very similar detection times at the specific volume they have been obtained, produce clearly different results when the system volume changes. The correct kinetics could thus be discriminated by simply repeating detection time experiments at different system sizes.

In conclusion, the two models developed and studied in this contribution allow to analyse in detail nucleation experiments at different initial conditions and with different temperature profiles. The models provide a general framework to describe the effect of volume on nucleation, while accounting also for crystal growth. Assuming scale-independent kinetics, they can be thus used to simulate the behaviour of the system at different volumes, thus gaining a better understanding of the effects of scaling-up. Thus, the two models allow to assess the feasibility of extrapolating kinetic information obtained in small, controlled volumes to larger values by directly comparing experimental data and simulation results at different scales.

General mathematical descriptions are necessary to understand better the physics of nucleation, and to obtain reliable kinetic parameters for process design and control. We believe that the models presented in this work can be a valid contribution toward the development of sound and reliable protocols for designing, analysing, and interpreting nucleation experiments.

Acknowledgements

The authors would like to thank Joop H. ter Horst and Somnath S. Kadam of the TU Delft for kindly providing the raw data of the TU Delft study² used in this work.

References

- 1 D. Kashchiev, D. Verdoes and G. van Rosmalen, *J. Cryst. Growth*, 1991, **110**, 373–380.
- 2 S. S. S. Kadam, S. S. a. Kulkarni, R. Ribera, A. I. A. Stankiewicz, J. H. J. ter Horst, H. J. H. Kramer and R. Coloma Ribera, *Chem. Eng. Sci.*, 2012, **72**, 10–19.
- 3 C. Lindenberg and M. Mazzotti, *J. Cryst. Growth*, 2009, **311**, 1178–1184.
- 4 O. Galkin and P. G. Vekilov, *J. Phys. Chem. B*, 1999, **103**, 10965–10971.
- 5 P. Laval, J.-B. Salmon and M. Joanicot, *J. Cryst. Growth*, 2007, **303**, 622–628.

-
- 6 M. Ildefonso, N. Candoni and S. Veessler, *Org. Process Res. Dev.*, 2012, **16**, 556–560.
 - 7 M. Ildefonso, N. Candoni and S. Veessler, *Cryst. Growth Des.*, 2013, **13**, 2107–2110.
 - 8 Z. Hammadi, N. Candoni, R. Grossier, M. Ildefonso, R. Morin and S. Veessler, *Comptes Rendus Phys.*, 2013, **14**, 192–198.
 - 9 S. Teychené and B. Biscans, *Cryst. Growth Des.*, 2011, 4810–4818.
 - 10 S. Teychené and B. Biscans, *Chem. Eng. Sci.*, 2012, **77**, 242–248.
 - 11 L. Goh, K. Chen, V. Bhamidi, G. He, N. C. S. Kee, P. J. A. Kenis, C. F. I. I. Zukoski and R. D. Braatz, *Cryst. Growth Des.*, 2010, **10**, 2515–2521.
 - 12 K. Chen, L. Goh, G. He, P. Kenis, C. Zukoski and R. Braatz, *Chem. Eng. Sci.*, 2012, **77**, 235–241.
 - 13 A. F. Izmailov, A. S. Myerson and S. Arnold, *J. Cryst. Growth*, 1999, **196**, 234–242.
 - 14 D. Knezic, J. Zaccaro and A. S. Myerson, *J. Phys. Chem. B*, 2004, **108**, 10672–10677.
 - 15 S. Jiang and J. H. ter Horst, *Cryst. Growth Des.*, 2011, **11**, 256–261.
 - 16 D. Randall, J. Nathoo, F. Genceli-Güner, H. Kramer, G. Witkamp and a.E. Lewis, *Chem. Eng. Sci.*, 2012, **77**, 184–188.
 - 17 S. a. Kulkarni, S. S. Kadam, H. Meekes, A. I. Stankiewicz and J. H. ter Horst, *Cryst. Growth Des.*, 2013, **13**, 2435–2440.
 - 18 R. Sullivan, R. Davey and G. Sadiq, *Cryst. Growth Des.*, 2014, **14**, 2689–2696.
 - 19 O. Pino-García and A. Rasmuson, *Ind. Eng. Chem. Res.*, 2003, **42**, 4899–4909.
 - 20 O. Pino-García and A. Rasmuson, *Cryst. Growth Des.*, 2004, **4**, 1025–1037.
 - 21 F. L. Nordström, M. Svärd and A. k. C. Rasmuson, *CrystEngComm*, 2013, **15**, 7285.
 - 22 Y. Huaiyu, A. Rasmuson and H. Yang, *Cryst. Growth Des.*, 2013, **10**, 4226–4238.
 - 23 M. Svärd, F. Nordström, E. Hoffmann and A. Rasmuson, *Cryst. Growth Des.*, 2013.
 - 24 M. Kuhs, J. Zeglinski and A. Rasmuson, *Cryst. Growth Des.*, 2014.
 - 25 D. Kashchiev, *Nucleation, Basic Theory with Applications*, Butterworth-Heinemann, 2000.
 - 26 C. Lindenberg and M. Krattli, *Cryst. Growth Des.*, 2009, **9**, 1124–1136.
 - 27 A. Randolph and M. Larson, *Theory of Particulate Processes*, Academic Press, London, 1971.
 - 28 D. Ramkrishna, *Population Balances: Theory and Applications to Particulate Systems in Engineering*, 2000, p. 355.
 - 29 D. Snyder and M. Miller, *Random Point Processes in Time and Space*, Springer-Verlag, New York, 1991, p. 481.